Cholesterol impacts chemokine CCR5 receptor ligand binding activity

Pierre Calmet, Christophe Cullin, Sandra Cortès, Maylou Vang, Nada Lepejova Caudy, Rim Baccouch, Jean Dessolin, Nada Taib Maamar, Sophie Lecomte, Bruno Tillier, et al.

Received Date : 16-Jul-2019

Revised Date : 27-Sep-2019

Accepted Date : 16-Nov-2019

Cholesterol impacts chemokine CCR5 receptor ligand binding activity

Pierre Calmet[1], Christophe Cullin[1], Sandra Cortès[2], Maylou Vang[1], Nada Caudy[1], Rim Baccouch[1], Jean Dessolin[1], Nada Taib Maamar[1], Sophie Lecomte[1], Bruno Tillier[2], Isabel D. Alves[1]

[1]CBMN, UMR 5248 CNRS, University of Bordeaux, Bat B14, allée Geoffroy St. Hilaire, 33600 Pessac, FRANCE

[2]Synthelis, 5 Avenue du Grand Sablon, 38700 La Tronche, FRANCE

Corresponding author: Isabel Alves, CBMN bat B14, allée Geoffroy St. Hilaire, 33600 Pessac, FRANCE; phone 0033540006849; email: i.alves@cbmn.u-bordeaux.fr

Running title: Cholesterol affects ligand binding to CCR5

Abbreviations: BCA, bicinchoninic acid assay; CGMDS, coarse grained molecular dynamics simulation; CHAPS, 3-[(3-cholamidopropyl)dimethylammonio]-1-propanesulfonate; CHS, cholesterol hemisuccinate; Chol, cholesterol; CMC, critical micelle concentration; DAPTA-FITC, D-Ala peptide T-amide-fluorescein isothiocyanate; DDM, dodecylmaltoside; DOPA, 1,2-dioleoyl-sn-

This article has been accepted for publication and undergone full peer review but has not been through the copyediting, typesetting, pagination and proofreading process, which may lead to differences between this version and the Version of Record. Please cite this article as doi: 10.1111/FEBS.15145

glycero-3-phosphatidic acid; DOPC, 1,2-dioleoyl-sn-glycero-3-phosphocholine; DOPE, 1,2-dioleoyl-sn-glycero-3-phosphatidylethanolamine; FA, Fluorescence anisotropy; GPCR, G-protein coupled receptor; HIV, Human Immunodeficiency Virus; IC_{50}, half maximum inhibitory concentration; IMAC, immobilized metal affinity column; K_D, dissociation constant; NTA, nitrilotriacetic acid; NTPs, nucleoside triphosphates; pATR-FTIR, polarized Attenuated Reflection Fourier Transform Infra-red; PMSF, phenylmethylsulfonyl fluoride; POPC, 1-palmitoyl-2-oleoyl-sn-glycero-3-phosphocholine; PWR, Plasmon Waveguide Resonance; R_{sat}, lipid/detergent ratio at which the liposomes start to solubilize; R_{sol}, lipid/detergent ratio at which the liposomes are totally solubilized; SUVs, small unilamellar vesicles; TCEP, tris(2-carboxyethyl)phosphine.

Keywords: Chemokine CCR5 receptor, cholesterol, *Pichia pastoris*, cell-free expression, plasmon waveguide resonance, fluorescence anisotropy.

Conflicts of interest: None declared.

Abstract

Background/Aims: The chemokine CCR5 receptor is target of maraviroc, a negative allosteric modulator of CCR5 that blocks the HIV protein gp120 from associating with the receptor, thereby inhibiting virus cellular entry. As noted with other GPCR family members, the role of the lipid environment in CCR5 signaling remains obscure and very modestly investigated. Controversial literature on the impact of cholesterol depletion in HIV infection and CCR5 signaling, including the hypothesis that cholesterol depletion could inhibit HIV infection, lead us to focus on the understanding of cholesterol impact in the first stages of receptor activation. **Methods:** To address this aim, the approach chosen was to employ reconstituted model lipid systems of controlled lipid composition containing CCR5 from two distinct expression systems: *P. pastoris* and cell-free expression. The characterization of receptor/ligand interaction in terms of total binding or competition binding assays was independently performed by Plasmon Waveguide Resonance and Fluorescence Anisotropy, respectively. Maraviroc, a potent receptor antagonist was the ligand investigated. Additionally, Coarse-grained Molecular Dynamics Simulation was employed to investigate cholesterol impact in the receptor conformational flexibility and dynamics. **Results:** Results obtained with receptor produced by different expression systems and using different biophysical approaches clearly demonstrate a considerable impact of cholesterol in the binding affinity of maraviroc to the

receptor and receptor conformational dynamics. **Conclusion:** Cholesterol considerably decreases maraviroc binding affinity to the CCR5 receptor. The mechanisms by which this effect occurs seems to involve the adoption of distinct receptor conformational states with restrained structural dynamics and helical motions in the presence of cholesterol.

Introduction

The chemokine receptor CCR5 belongs to the large G-protein coupled receptor (GPCR) family and is a drug target of tremendous interest as it is implicated in several pathologies including cancer and its metastasis, inflammatory diseases and neurological disorders. Moreover, CCR5, along with CXCR4 are co-receptors implicated in the process of HIV infection [1, 2]. In that sense, the receptor is the target of ligands that through receptor conformational changes aim at blocking different stages in the viral fusion process. One such ligand is maraviroc, the first CCR5 antagonist approved by both the European Medicines Agency (EMA) and the US Food and Drug Administration (FDA) for treatment of HIV-infected patients experiencing virological failure due to resistance to other classes of antiretroviral drugs [2, 3]. It represents a novel class of antiretroviral drugs, as it is the first therapeutic targeting a cellular rather than a viral protein. It is a potent negative allosteric modulator of CCR5 (IC_{50} of 2 nM) and potent antiviral agent (EC_{90} of 1 nM) [4] that prevents the HIV protein gp120 from associating with the receptor, thereby inhibiting virus cellular entry. A most recent report on the cryo-EM structure of the complex formed between CCR5, gp120 and CD4 provided important details about the structural parameters of the process [5]. Moreover, the high resolution structure of CCR5 bound to maraviroc and detailed description of the binding pocket has been reported [6].

Despite, the unquestionable contribution that such studies have provided at the fundamental level regarding the mechanisms underlying HIV fusion and at the therapeutic level concerning drug design strategies, one aspect that has remained controversial and underinvestigated concerns the role of the lipid environment in co-receptor action. More specifically, lipid domains rich in cholesterol and sphingomyelin (so-called lipid rafts) have been shown to modulate the activity of several GPCRs [7-10]. The increased concentration of such receptors in these domains may facilitate their intermolecular interactions and the ordered lipid environment may affect receptor functional

properties [11]. Different studies have suggested that cholesterol could play an important role in the process of viral fusion and CCR5 functioning. A report has shown that CCR5 requires membrane cholesterol to retain ligand binding and signaling functions and for HIV virion entry into cells expressing the co-receptors CCR5 and CXCR4, whereby its depletion would inhibit HIV entry [12]. It has also been revealed that cholesterol is important for chemotaxis of human neutrophils, but has no influence on early signaling by chemokine receptors on those cells [13]. The implication of rafts in the activation of CXCR4 by CXCL12 has further been shown in the context of prostate cancer [14]. Additionally, a study has shown that cholesterol depletion leads to failure of CCR5 to inhibit cAMP activity [15], therefore lipid action on the receptor can be present both at the level of the ligand but also of effector interactions, impacting receptor downstream signaling, internalization and desensitization. Whether the role of cholesterol arises from its individual properties alone or from the overall properties of the microdomains (rafts) where it is located remains largely unanswered. A study has shown that increasing cellular ceramide concentration can inhibit HIV infection [16]. Whether ceramide can prevent the ability to cluster chemokine receptors into microdomains and thus regulate their signaling remains to be investigated. Most studies aiming at investigating the role of cholesterol were rather indirect, relying on depletion experiments using β-cyclodextrin or the use of cholesterol reducing drugs (filipin, nystatin) and/or monitoring changes in cell surface binding profiles by using receptor-specific antibodies. Herein, we have set to understand the impact of cholesterol in the first stage of the process, that is the ligand-binding to the CCR5 receptor leading to its activation. To discard any controversy on cholesterol depletion procedures [17], we have rather employed an approach relying on the use of reconstituted receptor model membranes of totally controlled lipid composition. For such, two alternatives were employed: receptor expression in *P. pastoris* followed by detergent-isolation, purification and reconstitution in liposomes; cell-free expression of the receptor with *E. coli* cellular machinery concomitantly performed in the presence of liposomes allowing direct insertion of the receptor into such lipid system. To determine ligand binding affinity to the receptor and cholesterol impact in such interaction, plasmon waveguide resonance (PWR) and fluorescence anisotropy (FA) measurements were conducted on the two types of samples. The results demonstrate that the presence of cholesterol in the membrane significantly impacts maraviroc binding

to the receptor and shed light on the role of cholesterol in receptor conformational changes and dynamics.

Results

Solubilisation of CCR5 from *P. pastoris* membranes and purification

Following CCR5 expression by *P. pastoris*, cells were disrupted by mechanical forces and membranes isolated using classical centrifugation approaches (see Experimental Section for details). Total protein content in membrane fraction was quantified by a bicinchoninic Acid (BCA) assay indicating yields of about 60 mg of total of protein per L of culture. Membrane aliquots were stored at -80°C for further use.

As the main aim of the current project is to determine the impact of membrane cholesterol in the ligand binding activity of CCR5, receptor isolation and reconstitution in model lipid systems of controlled lipid composition is required. Indeed, while mammalian systems can be enriched (by addition of specific fatty acids in the culture medium during cell growth, allowing for phospholipid enrichment following lipid esterification [18]) or depleted in certain lipids (for example cholesterol depletion by incubation with β-cyclodextrin [17]), bypassing the need for receptor isolation and reconstitution procedures, the literature on this subject regarding *P. pastoris* is rather nonexistent. Moreover, in the specific case of cholesterol, the use of β-cyclodextrin for cholesterol depletion has been associated with unwanted cellular effects [17]. Additionally, this procedure requires a lipid quantification step to accurately determine the lipid membrane composition surrounding the receptor of interest. In contrast to mammalian cells, yeast cells contain ergosterol instead of cholesterol. Although both sterols are found in membranes and serve common functions such as lipid raft formation, they do not share the same chemical properties and make unicellular fungus as *P. pastoris* very unlikely to study the role of cholesterol on ligand binding activity of CCR5 (although some mutants have been engineered to produce cholesterol [19]). Therefore, while the use of reconstituted model systems is a rather long and complicated process including both receptor isolation, purification and reconstitution procedures, it has the advantage of providing total control and knowledge of the lipid membrane composition. In addition, different lipid model systems (liposomes, planar lipid

membranes, nanodiscs, etc) can be prepared depending on the biochemical, biophysical approach used afterwards for the characterization of the receptor activity.

Solubilisation of *P. pastoris* membranes expressing the CCR5 was performed with a mixture of two detergents, dodecylmaltoside (DDM) and CHAPS and a cholesterol analog (cholesterol hemisuccinate, CHS), reported to improve receptor stability during detergent-isolation procedures [20-22] and to increase the amounts of solubilized material [23] for other GPCRs and the CCR5 itself [24]. Additionally, a CCR5 partial agonist, J113863, was included during the solubilisation step to improve receptor stability. The ratio used was 1%/0.1%/0.02% (DDM/CHAPS/CHS), a mixture that in the case of DDM is well above the CMC (critical micelle concentration) ensuring the presence of detergent micelles, essential for receptor solubilisation. The presence of the solubilized receptor in the different stages of the solubilisation process was followed by Dot-Blot assay with the use of anti-His antibody. This allowed for the optimization of the ratio of total protein versus quantity of immobilized metal affinity column (IMAC) resin, protein incubation time and establishment of imidazole gradient. As presented in Fig 1A, the established protocol (described in the Experimental Section) allowed for the receptor to be recovered after imidazole elution with negligible lost (point 3 on the Dot Blot). The solubilized receptor is then purified by batch with the use of a metal affinity column (Nickel-nitrilotriacetic acid, NTA) that includes overnight incubation with beads following by batch elution with a gradient step of imidazole (details found in the Experimental Section). The concentration of detergent is decreased in the elution step to 0.1%/0.1%/0.02% (DDM/CHAPS/CHS) to facilitate the reconstitution procedure performed afterwards. The identity and purity of the receptor prepared by such approach can be appreciated from the Western Blot and SDS gel analysis in Fig. 1B and C. The receptor band corresponds to that observed at around 50 KDa. This is superior to the reported MW of the receptor 40.6 KDa [25], the difference could be explained by the presence of post-translational modifications in the sample.

Reconstitution of the detergent-solubilized and purified CCR5 in lipid model systems

Reconstitution of functional CCR5 in liposomes, starting from detergent-solubilized and purified forms and the use of either dialysis or Bio-beads to remove detergent excess, has been reported [26, 27]. In our work, various procedures were assayed for the reconstitution of the detergent-solubilized

CCR5 in both solid supported lipid bilayers or small unilamellar vesicles (SUVs) including the detergent dilution approach whereby the detergent dilution in the receptor sample is decreased below CMC of the detergent mixture and the use of Bio-beads to remove excess of detergent. For the establishment of the best conditions for the reconstitution process, we have followed the evolution of POPC (1-palmitoyl-2-oleoyl-sn-glycero-3-phosphocholine) solubilisation (SUVs in this case) by incremental addition of detergent. Turbidity measurements at different lipid/detergent ratios allow to follow this process and the determination of R_{sat} (lipid/detergent ratio at which the liposomes start to solubilize) and R_{sol} (lipid/detergent ratio at which the liposomes are totally solubilised) as described by Rigaud and Levy [28]. The best stage for receptor reconstitution is located between the onset of solublisation (R_{sat}) and the complete solubilisation of liposomes (R_{sol}). While such values are known for the case of DDM, they aren't for the current situation where a mixture of three detergents is used. R_{sat} and R_{sol} of 0.97 ± 0.03 and 1.7 ± 0.08, were respectively obtained from the slope of the two lines presented in Fig. 2. While this information was used to optimize the reconstitution process, the results were not satisfactory as no receptor or very small amounts were reconstituted in the model systems. Moreover, in the case of reconstitution in SUVs, the proteoliposomes formed upon reconstitution were quite unstable in terms of their supramolecular assembly and the receptor quickly lost its activity. We have thus developed an alternative solution that we called one-pot purification and reconstitution assay. It consists in performing both the liposome reconstitution and imidazole elution simultaneously in the column containing the Ni-beads bound to the detergent-solubilized CCR5. Following elution from the column, to improve the homogeneity of the recovered proteoliposomes, they are passed through a 100 nm filter system. This procedure was found valuable to increase sample homogeneity, a parameter that is important to improve the quality of FA measurements to be performed to follow ligand-receptor interaction (as presented below) but also found to contribute to increase sample stability over time. Details of the protocol can be found in the Experimental Section. To ascertain that the reconstitution procedure was successful the following aspects need to be validated: 1) a proper lipid membrane can be formed by the fusion of such proteoliposomes with a surface (silica or germanium, used for PWR and pATR-FTIR measurements, respectively); 2) the receptor is present in the lipid membrane with proper orientation; 3) the receptor responds to ligand binding with affinities that correlate with those reported in the literature from classical cellular

binding assays. Our approaches to validate the different parameters were: pATR-FTIR (for aspects 1 and 2), PWR and FA (indirectly for aspect 2 and directly for aspect 3). Regarding aspects 1 and 2, pATR-FTIR was used as both lipids and proteins possess inherent specific non-overlapping absorption bands in IR. Moreover, the measurement of ATR-FTIR spectra with polarized light, both *p*-(parallel to the incident light) and *s*-(perpendicular to the incident light) polarizations, allowed to determine the anisotropy and orientation of both components relative to the crystal surface onto which the bilayer is formed (germanium in this case). All those aspects are further described below.

Cell-free expression and liposome reconstitution of CCR5

Cell-free expression offers a promising alternative method to produce membrane proteins. Cell-free expression systems exploit the cell transcription and translation machinery outside of the cells to express only the protein of interest. Cell-free systems offer many advantages due to their open nature, unlike cell-based systems where the cells constitute closed units.

The flexibility of an open system allows the expression of membrane proteins in the presence of defined and preformed liposomes. Then, these membrane proteins can be translated directly into appropriate hydrophobic environment offering significant benefits for the functional folding of the synthesized proteins. Cell-free expression has successfully been applied to GPCR production [29-31]

The main objective of this study being to determine the impact of membrane cholesterol in the ligand binding activity of CCR5, we produced CCR5 in the presence of liposomes with or without cholesterol.

The cell-free reaction was incubated with intensive agitation at 20 °C. For each new protein target parameters like the concentrations of critical compounds might need to be optimized in order to find the best conditions for high level expression. After adjusting magnesium and potassium ions concentrations, the expression efficiency was determined by Western blot, using anti-histidine antibody, and quantified by Coomassie brilliant blue staining (Figure 3). The batch expression yield of the partially purified proteoliposomes ranged from 30 to 45 µg/mL of cell-free mixture. This value was estimated by comparison with the BSA lanes in Fig. 3B.

The selection of suitable membrane compositions was a crucial point. Parameters such as lipid size, charge and resulting membrane topology had to be carefully studied for the membrane insertion and

an efficient folding of membrane proteins. The composition of liposomes was determined by a previous study [32]. As we can see on Figure 3B, the expression yield is not affected by the presence of cholesterol into liposomes.

Ligand binding activity of CCR5 and cholesterol impact

CCR5 from *P. pastoris* reconstituted in a POPC versus POPC/chol (9/1 mol/mol) membrane

The presence of the receptor in the liposomes can be indirectly proven by the interaction of ligand with the proteoliposomes that was monitored independently by two approaches, PWR and FA. The addition of liposomes to the PWR sensor surface results in increase in the resonance minimum position of both *p*-and *s*-polarized light (~230 and 120 mdeg for *p*- and *s*-pol, respectively) (Fig. 4A, B). Such values are above what is expected for a pure lipid membrane, so additional mass should be present that could be explained by the contribution of the receptor presence in the system. Moreover, the signal is quite anisotropic (with shifts much higher for *p*- than *s*-pol) indicating that the molecules immobilized in the sensor surface are anisotropic (this is the case of lipids and GPCRs that could be generally described by a cylinder-type shape) and oriented with the long axis perpendicular to the sensor surface (and along the *p*-pol axis). The incremental addition of ligand to the proteolipid system leads to further spectral changes, indicating that the ligand is interacting with the deposited proteolipid membrane (Fig. 4A, B). Indeed, resonance angle shifts to higher values are observed for both polarizations upon ligand addition. In view of the fact that the ligand being added has a very low molecular weight (513.7 g/mol) and that its concentration is quite low in the cell sample (maximum concentration is of 10 nM), its contribution to changes in the refractive index are completely negligible. Therefore, the observed spectral changes can only be attributed to ligand-induced receptor conformational changes. Such scenario has already been observed in previous PWR experiments involving ligand interaction with GPCRs [33-36]. From PWR experiments, it was possible to determine a binding affinity of 0.8 nM between maraviroc and the CCR5 (Fig. 4C), that is in very close agreement with reported values from the literature from cellular binding assays [37]. In parallel, the proteoliposomes were tested for their ability to bind and compete with CCR5 ligands by FA, an approach that has been reported to be of great use to characterize such interactions [38]. For such assay, a CCR5 fluorescent antagonist (DAPTA-FITC; D-Ala peptide T-amide-fluorescein

isothiocyanate) was used at fixed concentration and variable concentrations of maraviroc (from 10^{-13} to 10^{-4} M) were added to allow for binding competition with the fluorescent ligand for the receptor binding site. The experiment allows one to obtain an IC_{50} (the half maximum inhibitory concentration) for the process that provides a measure of the receptor/ligand affinity. Using this parallel assay, similar affinities were obtained (Fig. 4D) which further proves that the CCR5 receptor produced by *P. pastoris* and reconstituted in the POPC model membranes is active in terms of ligand recognition.

The understanding of the role of cholesterol in CCR5 ligand recognition remains the main objective of this study. Therefore, the same experimental approaches were applied to proteolipid model membranes containing cholesterol (10% molar ratio). PWR results surprisingly show that ligand addition to the proteolipid membrane results in no spectral changes, even at high ligand concentration (final concentration in the cell being over 1 μM) (Fig. 5A, B). The possibility of receptor absence in the sample due to improper reconstitution in the membrane in the presence of cholesterol was raised. To confirm the presence of receptor in the cholesterol-containing liposomes and the lipid membrane formed upon liposome fusion, polarized ATR-FTIR experiments were performed (as described above). Following proteoliposome (composed of POPC and cholesterol at 9/1 mol/mol ratio and the CCR5 receptor) fusion with the ATR germanium crystal, the IR signal was acquired with both *p*- and *s*-polarized light and the regions corresponding to lipid (from 2800 to 3000 cm^{-1}) and amide absorption (1500-1700 cm^{-1}) were monitored and analyzed. Figure 6 shows the *p*- and *s*- polarized ATR-FTIR spectra in two ranges at high wavenumber (3050-2750 cm^{-1}) and at low wavenumber (1800-1450 cm^{-1}). The lipid marker bands are observed at 2925 and 2850 cm^{-1} assigned to the $\nu_{as}CH_2$ and ν_sCH_2, respectively attesting the presence of lipids on the germanium crystal. The band at 1740 cm^{-1} is also a signature of the presence of phospholipid, more precisely assigned to the C=O stretching mode of the ester group present in the POPC. The intensity absorbance of 1.3×10^{-3} for the band at $\nu_{as}CH_2$ on *p*-ATR-FTIR spectrum is characteristic of formation of one intact lipid bilayer. The position of the $\nu_{as}CH_2$ band at 2925 cm^{-1} is indicative of some disorder in the chains that could arise from the presence of traces of detergent in the membrane. The dichroic ratio of the ν_sCH_2 band at 1.6 allows to estimate the average C-C-C angle of the lipid carbon chains at 58° with the normal at the interface, as described by Castano and Desbat [39]. The bands observed at 1655 and 1550 cm^{-1}

assigned to amide I and II vibrational modes reveal the presence of CCR5 protein in the lipid bilayer. CCR5 is mainly organized in α-helical structure, as revealed by the amide I position at 1655 cm^{-1}. The dichroic ratio of the amide I band at 1.75 indicates a tilt of the α-helices of around 40° relative to the normal at the interface [39]. Therefore, the experiments demonstrate that the lipid membrane is properly formed and that the receptor is reconstituted in this membrane with a certain degree of the expected orientation. Therefore, FA experiments were performed in such samples as another approach to characterize ligand receptor affinity. As shown in Fig. 5C, one can see a nice binding competition response between the two ligands that allowed us to determine an inhibition constant for the process. The affinity observed (23 nM) was much lower than that observed in the absence of cholesterol (0.8 nM) thus indicating that cholesterol changes the properties of the receptor considerably.

A summary and comparison of the ligand binding affinity to CCR5 obtained from FA and PWR from at least three independent experiments are respectively presented in panels A and B of Figure 7. In the absence of cholesterol in the membrane binding affinities between the two measurements are very much comparable. To note that the presence of cholesterol in the membrane leads to a 30-fold decrease in binding affinity.

CCR5 from cell-free expression and directly incorporated into a (DOPC/DOPE/DMPA/chol) versus (DOPC/DOPE/DMPA) membrane

Similar experiments to those reported above were performed with CCR5 that was produced by cell-free expression with concomitant reconstitution into liposomes composed of either (DOPC:DOPE:DMPA:chol; 1.9:1:1.2:1.9 molar ratio) or (DOPC/DOPE/DMPA; 1.9:1:1.2 molar ratio) To note some major differences between the two samples regarding the protein and lipid content: 1) the CCR5 produced by *P. pastoris* was isolated and purified before the reconstitution process, therefore the proteoliposomes and proteomembranes contain negligible contaminant proteins as the SDS electrophoresis indicates (Fig. 1C). This is not the case for the proteoliposomes produced from CCR5 cell-free expression, which are purified on discontinuous sucrose gradient. This purification technique does not remove all contaminant proteins contained in the bacterial extract thus part of the components of the reaction mixture are present in the proteoliposomes. 2) The composition of the model lipid system is different in the two cases: for the studies with the purified and

reconstituted CCR5 from *P. pastoris*, the lipid membrane was solely composed of POPC or POPC/cholesterol and the cholesterol content was 10% (mol/mol). For the studies with the cell-free expression sample, the lipid content was a complex mixture of several lipids: DOPC, DOPE and DMPA with or without cholesterol, and the cholesterol content was 30% (mol/mol). Another difference regards the liposome average size from the two different systems, that is rather small (≤ 30 nm) for the reconstituted sample and quite large (250-600 nm) for the proteoliposomes produced from cell-free expression. The preformed liposomes tend to fuse during the cell-free reaction.

As in the case of proteoliposomes obtained from *P. pastoris*, the fusion of the proteoliposomes from cell-free expression on the PWR sensor surface resulted in a large and anisotropic response (about 220 and 180 mdeg observed for the *p*- and *s*-pol response, respectively) (Fig. 8A, B). The magnitude of the response is quite comparable to that observed by PWR (as described above) but less anisotropic, probably due to the presence of less anisotropic proteins in the sample besides CCR5. The formation of a proteolipid membrane was also followed by pATR-FTIR and results obtained demonstrate both the presence of a properly oriented lipid membrane and of a high protein content (data not shown). Despite the fact that the sample possesses many other proteins than the CCR5, maraviroc addition resulted in PWR spectral changes and a saturating response (Fig. 8C) when cholesterol was absent. This shows that for this type of PWR experiments, receptor purity is not essential. In terms of the receptor response to the ligand, two aspects in the binding curve can be analyzed and compared among experiments: the magnitude of the response (maximum PWR shift obtained upon saturation) and the anisotropy of the response (the relative *p*- and *s*-shifts observed upon saturation). While differences in the magnitude of the response can result both from different amounts of receptor in the sample and/or different ligand-induced conformational changes of the receptor, anisotropy differences in ligand response must be ascribed to different receptor conformational changes. Considering that there are major differences in proteoliposome preparation between the reconstituted and cell-free samples, one cannot conclude regarding the subtle differences in the magnitude of the response observed in the two experiments. But, it is quite clear when comparing Fig. 4C and Fig. 8C that the anisotropy of the receptor conformational change upon ligand addition is different (being quite anisotropic in the first case and isotropic in the second one). This indeed points to the idea that the receptor conformational change is different in the two cases, a fact

that can result from either or both differences in receptor and lipid composition of the sample. Another aspect that quite differs between the two samples regards the ligand binding affinity that is considerably lower for the protein produced from cell-free expression (7-10 nM for the two approaches used, PWR and FA) than that produced by *Pichia* and reconstituted in the model membranes (Fig. 7 and 9). This could again originate either from the quality of the protein produced and/or the lipid environment. Nonetheless, both approaches are efficient in producing high quality receptor able to recognize ligand with affinities that are comparable to values reported in the literature obtained from classical cellular ligand binding assays.

When similar experiments were performed in the presence of cholesterol (30% molar ratio) in the membrane, the affinity for maraviroc dropped to about 200 nM indicating that cholesterol negatively impacts ligand binding to CCR5. Again, no PWR spectral changes could be measured upon ligand binding to the sample as previously indicated (data not shown). Cholesterol impact observed in the receptor obtained from different expression systems and distinct reconstitutions procedures leads to comparable results, despite the differences in the cholesterol content in the two samples (10 versus 30% for the reconstituted *P. pastoris* sample versus the cell-free system) and some differences in other phospholipid contents regarding the headgroup nature (presence of PA and PE phospholipids).

Cholesterol impact in the CCR5 dynamics – CGMDS

Experimental studies presented showed that membrane cholesterol impacts the properties of CCR5 leading to a decrease in the ligand binding activity, this process can be related to the protein conformational changes and dynamics. To support these results, coarse grained molecular dynamics simulations (CGMDS) is useful because it offers the possibility to study the evolution of large systems over time in a timescale up to the microsecond or even the millisecond. Moreover, the use of such digital simulation technique allows to look into biomolecule dynamics and conformational changes and to analyze the interaction of cholesterol molecules with the protein. CGMDS aimed at determining the impact of cholesterol in the receptor conformational flexibility and dynamics, particularly whether there are preferred transmembrane (TM) helices that are contacted by cholesterol. To answer that, the receptor was embedded in two lipid systems (in the absence – POPC; and in the presence of cholesterol – POPC with 10% cholesterol) to observe the influence of

cholesterol in CCR5 dynamics (Fig. 10). Dynamics were carried out in aqueous medium and at saline concentration (0.15 M). Two replica of each system were simulated for 4 μs each.

The evolution of the protein structure was analyzed by computing the root mean square deviation (RMSD) between the structure during the simulation and the initial one. Only the beads representing CCR5 backbone were taken into account in the calculation and these results are presented in figure 11A. The RMSD revealed significant fluctuations of the protein in the absence of cholesterol in the membrane, testifying CCR5 dynamics in such condition. When 10 % of cholesterol was added, upon cholesterol/receptor contacts a considerable loss of mobility and thus a decrease in the RMSD was observed along distinct fluctuations (Fig. 11A). Going deeper in the analysis in terms of each individual helix, the more flexible helices for the two systems were determined to be TM helices V, VI, VII and I which proved really dynamic, with high RMSD values and variations (Fig. 11B). As it can be appreciated from the data, the presence of cholesterol impacts TM helix dynamics with a lowering in the RMSD observed for these helices. Such effect was predominantly marked for helices II and IV.

The radial distribution functions (RDF) of sterol molecules with respect to each helix was determined which allows to identify potential preferentially contacted helices. According to data presented in Figure 12A, TM helices VII, V, VI, IV and even I are involved in the cholesterol-protein interactions. These helices have been identified as cholesterol occupancy sites in others GPCRs [40-44]. Transmembrane segments already reported as cholesterol binding sites [45] were also found as highly probable sites all along the course of our simulations. In particular, helix I F43-K59, helix IV T143-I151, helix V L207-K219 and helix VI F238-L257 showed a greater interaction than helix VII C291-A298 (Fig. 12B). This latter segment, while previously described as an essential player [44], in our study the CCR5 conformational state did not seem as important, probably because the cholesterol level in our simulations was only 10% compared to the 30% used by Gahbauer et al. The fact that no ligand was present in the orthosteric site during the simulations discussed here could also explain the discrepancy.

Discussion

Cholesterol impact in the pharmacology of some GPCRs has been investigated using biochemical and biophysical approaches. Cholesterol can exert its impact both indirectly, by modulating the membrane bulk properties as membrane fluidity, curvature, lateral pressure and bilayer thickness or indirectly *via* binding to specific cholesterol binding sites in the receptor [43] or both. Atomistic molecular dynamics (MD) simulations have identified multiple cholesterol binding sites on the surface of GPCRs, the occupancy of which resulted in increased conformational stability [42, 43, 46, 47]. Using molecular docking, putative cholesterol binding sites for the CCR5 receptor have been revealed [44]. CGMDS have revealed cholesterol to impact GPCR dimerization processes, including kinetics and dimer interface [48, 49]. Selent and collaborators have reported following both experimental and computational studies that cholesterol can enter the adenosine A_{2A} receptor ($A_{2A}R$) binding pocket from the membrane milieu through a gate used for opsin ligands [46]. Yet, another recent study on this same receptor, revealed a certain correlation between the strength of lipid contacts, including cholesterol, and the degree of dependence on the receptor conformational states, suggesting lipids to regulate receptor conformational dynamics [50]. Studies on cholesterol impact on CCR5 activation and pharmacology by a direct method using theoretical MD or other biophysical approaches in lipid membranes whose lipid composition is tightly controlled are still missing. In view of the fact that some indirect studies, either based on cholesterol depletion (by β-cyclodextrin) or cholesterol reduction by drugs (filipin, nystatin), have indicated a potential role of cholesterol in CCR5 signaling and HIV infection [51, 52], we have set to directly investigate cholesterol impact in the first signaling event, that is ligand binding to the receptor and consequent receptor conformational changes. Previous data from our group suggested cholesterol to have an impact in receptor/ligand affinity, nonetheless such studies were quite preliminary and performed with and engineered CCR5 thermostable mutant, rather than the wild type form [33]. The present work, performed with wild type CCR5 produced via two alternative and completely independent sources, *P. pastoris* and cell-free expression, simultaneously reveals cholesterol to significantly impact maraviroc affinity to the receptor with a 20 to 30-fold decrease in affinity when cholesterol is present in the membrane. While, one can argue that the impact in binding affinity is rather modest, very minor differences in receptor/ligand affinity have been shown to highly impact the selectivity of the activated signaling cascades in the case other chemokine receptors as the CXCR3 [35]. This demonstrates the extremely thin fine-tuning of GPCR

activation and signaling. Moreover, both the fact that receptor-conformational changes could not be followed by PWR in the presence of cholesterol while they could in the absence of cholesterol and the fact that CGMDS reveals a decrease in receptor conformational flexibility suggests that cholesterol modulates the receptor dynamics and magnitude of ligand-induced conformational changes. A decrease in CCR5 dynamics could be responsible for the observed decrease in ligand affinity to the receptor in the presence of cholesterol due to modifications in the kinetics of ligand recognition. Indeed, due to increased TM helix rigidity in the presence of cholesterol, ligand-induced receptor conformational changes could be affected either in terms of the time needed to recognize the receptor or the time the receptor stays in each receptor sub-conformation. Our results regarding cholesterol impact are in agreement with a previous report from the Vattulainen group on the β_2-adrenergic receptor, that by the use of atomistic modulation demonstrated the allosteric regulation of receptor due to modulation in conformational variability. The study shows that cholesterol, and to a less extent its analogues, bind to receptor binding sites and impede receptor structural flexibility [42]. While such studies are purely theoretical, experimental evidence by FRET studies on cholesterol effect in the conformational states of another GPCR, the oxytocin receptor, and revealed a more compact receptor state in the presence of cholesterol [53].

As CCR5 is one of the co-receptors for HIV infection, along with CXCR4, a parallel can be established between the observed cholesterol impact in ligand recognition by CCR5 and the influence of cholesterol on CCR5 recognition by chemokine CCL4 [52, 54] and anti-CCR5 antibodies [52, 54, 55] as well as cholesterol impact in fusion mediated by CCR5-using HIV envelope glycoprotein (Env) [12]. From the reported data, we can suppose that cholesterol-induced decrease in maraviroc binding affinity to CCR5 might rather be expected for the reasons presented below. In a simplistic manner, one can consider two main conformations of CCR5: one associated with low content or in the absence of cholesterol, and another one associated with higher content of cholesterol [52, 55]. The cholesterol-dependent conformation of CCR5 is associated with more efficient binding of chemokine CCL4 [52, 54] and conformation-dependent anti-CCR5 antibodies 45523 [52, 54] and 45531 [55], as well as more efficient fusion mediated by CCR5-using HIV Env [12]. The cholesterol-dependent conformation can be named active, whereas cholesterol-independent conformation can be named inactive [55]. On the other hand, maraviroc is an inhibitor of HIV entry and, moreover, maraviroc

binding to CCR5 prevents it from binding the chemokine CCL3 [56], and several lines of evidence suggest that maraviroc stabilizes CCR5 in an inactive conformation [6]. Hence, both absence (or low content) of cholesterol and maraviroc binding are associated with inhibited fusion mediated by CCR5-using HIV Env, lower chemokine binding to CCR5 and inactive CCR5 conformation. We can conclude that higher maraviroc binding to CCR5 might be expected to be associated with the lower content of cholesterol in the CCR5-containing membranes.

The present study further demonstrates the importance of using parallel experimental approaches, with no ligand binding being observed by PWR due in principle to the rather limited magnitude of the receptor conformational changes, while under such conditions ligand binding and competition were observed by FA measurements.

Comparable binding affinities were observed for CCR5 produced by *P. pastoris* and cell-free expression. Therefore, the study validates the two different expression systems used: *P. pastoris*, a system that has been reported successful for the expression of several GPCRs [57-59] and cell-free expression approaches with concomitant receptor incorporation into lipid model systems. It should be noted that a major difference between the two expression systems regards the capacity for each system to produce post-translational modifications (PTMs) in the receptor. While, *P. pastoris* is able to produce most PTMs, this is not the case of cell-free expression from *E. coli* lysates. Nonetheless, for the studies involving ligand-receptor interaction herein performed, PTMs do not seems to really impact as binding affinity differences are not very large. Certainly, both approaches possess advantages and inconveniences. Regarding cell-free expression, the direct incorporation of the protein in a controlled lipid membrane environment allows for a quick route to obtain properly folded proteins in such environment, bypassing the long and demanding process of protein reconstitution that is required when classical eukaryotic or prokaryotic expression is used. The presence of sample impurities when using cell-free expression approaches can be deducted by performing similar experiments using proteoliposomes containing bacterial extract impurities in the absence of the expressed protein of interest. If indeed contaminants in such sample are problematic, then cell-free expression can be performed in the presence of detergents and so receptor can be then purified by classical approaches. The present study shows that receptor purification procedures could be bypassed, at least for the measurements of ligand/receptor interaction by the approaches herein used.

While the potential impact of cholesterol in receptor conformation and dynamics suggests cholesterol impact to propagate beyond ligand-receptor interaction, that remains yet to be proven. A very recent report on the impact of cholesterol on both ligand binding and cAMP signaling by the $A_{2A}R$, shows that while ligand binding is not affected by membrane cholesterol content, cAMP response is reduced following membrane cholesterol depletion [60]. Atomistic simulations by the authors suggested that cholesterol interacts specifically with a receptor consensus motif when the receptor is in an active state, but not when in an inactive state. Future work to reveal the molecular details on the cholesterol impact in CCR5 conformation in the absence of ligand and in the presence of different classes of ligands should help decipher the molecular mechanisms of cholesterol/receptor interactions. The study of cholesterol impact in the different signaling cascades activated by the receptor should answer to the question whether such impact propagates downstream in the signaling cascade leading towards a biological response, closing the loop between cholesterol impact in receptor activation/conformation and CCR5-mediated HIV infection. Therefore, a potential adjuvant therapeutic interest of controlling cholesterol content in the CCR5 receptor vicinity remains to be investigated.

Materials and Methods

Materials

Lipids were purchased from Avanti Lipids. Salts, buffers and solvents were purchased from Sigma-Aldrich. The ligand maraviroc was from Tocris. Yeast extract, Bacto peptone were from Biokar diagnostics. Yeast Nitrogen Base (HMW) was from Thermo-Fisher scientific. Biotin, PMSF, TCEP, protease inhibitor cocktails were from Sigma-Aldrich. The detergents used for CCR5 solubilisation were purchased from Thermo-Fisher scientific. The Poly-Prep® Chromatography Column was purchased from Bio-rad. The HIS-Select® Nickel Affinity Gel and imidazole used for CCR5 purification and elution was from Sigma Aldrich.

HEPES, nucleoside triphosphates (NTPs), magnesium glutamate, potassium glutamate, amino acids, chaperones, sucrose were from Sigma-Aldrich. Poly histidine antibody conjugated with a horseradish peroxidase was purchased from Sigma-Aldrich.

Construction of the plasmid and transfection into *P. pastoris*

pPIC9K_MP2_NPFFR2 (kindly provided by Dr. R. Wagner) was cut by *BamHI* and *EcorI*. CCR5 ORF (provided by Dr. N. Tschammer) was amplified from by PCR using 5'-GCGTTTAAACTTAAGCTTGGTACCGAGC-3' and 5'-GTACAGGTTTTCGAACAAGCCCACAGATATTTCCTGC-3' and cut by *BamHI*. After ligation and heat inactivation, the linearized plasmid was eluted from 0.8% agarose gel and reannealed using the Gibson Assembly kit (New England Biolabs, USA). The resulting plasmid pPIC9K-CCR5 allows for expression of a chimeric protein that contains an N-terminal α-factor signal sequence from *S. cerevisiae* followed by a Flag-tag, a decahistidine-tag, a tobacco etch virus (TEV) protease site, CCR5 ORF, another TEV protease site and the biotinylation domain from *Propionibacterium shermanii* at the C terminus [59]. The protease-deficient *P. pastoris* strain SMD1163 (his4, pep4, prb1) (Invitrogen) was used for transformation by electroporation according to reported protocols [61] followed by selection for G418 resistance due to integration of the plasmid in the genome. Several clones were tested for CCR5 expression and showed the same level of expression. One of them was further used for biochemical analysis.

Protein extraction

CCR5 expression by *P. pastoris,* cell lysis and isolation of the membrane fraction

The clone selected for CCR5 expression was grown overnight in 75 mL of BMGY medium (1% Yeast extract, 2% Bacto peptone, 100 mM phosphate buffer (13.2 mM K_2HPO_4; 86.8 mM KH_2PO_4) at pH 6, 1.34% Yeast Nitrogen base, 0.00004% Biotine and 1% Glycerol). This pre-culture was added to 1L of BMMY (same as BMGY with 0.5% of methanol instead of glycerol) to get an initial OD_{600} of 1 and grown under strong agitation at 30°C. Then *Pichia* culture growth is monitored by OD measurement and when saturation is reached (OD of about 16-22; usually within 24h), cells are centrifuged for 45 min at 4000 × g. If the culture is not yet at saturation, an additional 0.5% Methanol is added and culture left for additional 24h or until the optimal OD is reached. The pellets are collected, resuspended in lysis buffer (50 mM Tris-HCl pH 8, 500 mM NaCl and 5% glycerol; 2×40 mL per L of culture) and transferred to 50 mL Falcon tubes. The tubes are centrifuged at 12000 × g for 5 min and pellet collected. Usually about 12 g/L of culture is obtained. The pellet is then resuspended in the enriched lysis buffer (50 mM Tris-HCl pH 8, 500 mM NaCl and 5% glycerol, 1

mM PMSF, protease inhibitor cocktail without EDTA at advised concentration), usually 80 mL per L of culture. The lysed culture solution is separated in 50 mL Falcon tubes and 10 mL of glass beads are added per flask.

Cells are then disrupted by mechanical force using glass beads and a homogenizer (MP-FastPrep, MP Biomedicals). To do so the instrument block where tubes (containing about 20 mL of cells and 10 mL of glass beads) are to be placed is previously cooled down to -20°C and small amounts of dry ice are added around the tubes to maintain the temperature in the sample as low as possible. Two cycles of 30 sec (6 m/s) are run intercalated by 5min pause to let the sample cool down in ice bath. After this step, each tube is centrifuged at 1000 × g for 5 min, the supernatant collected and the procedure repeated once again. The supernatants are combined and centrifuged again at 2000 × g for 5 min to remove excess of cell debris and intact cells. The supernantant is collected and centrifuged at 18000 × g for 1h to obtain the membrane fraction (pellet). The pellet corresponding to the membrane fraction is then resuspended in the enriched lysis buffer (6 mL per L of culture) and the total protein concentration is measured by a BCA assay following the furnished protocol (BCA protein Assay Kit, Pierce). Samples of 1 mL at 10 mg/mL are prepared and stocked at -80°C until further use.

Solubilisation of the membrane fraction from *P. pastoris* expressing CCR5 and receptor purification

For each batch of CCR5 prepared, 1 mL of membrane fraction (10 mg/mL of total protein) is used. The frozen aliquot is slowly unfrozen in an ice bath and resuspended in 9 mL of solubilisation buffer (50 mM Tris-HCl, 150 mM NaCl, 5% glycerol, 1% DDM, 0.1% CHAPS, 0.02% CHS, 1 mM PMSF, 0.1 mM TCEP and 1 µL/mL of protease inhibitor cocktail from Sigma). To note that protease inhibitors and reducing agents are freshly added. Additionally, we have found that the inclusion of a CCR5 ligand during the solubilisation process helps the receptor to keep its activity. A low affinity ligand (J113863, Tocris) was included at 100 µM, so that it would be less likely to interfere with the ligand binding assays performed afterwards to follow receptor activity. The sample is resuspended with the use of a pipette or a Potter type homogenizer to ensure proper solubilisation and incubated for 30 min at 4°C. To separate any non-solubilised material, the sample is then centrifuged at 18000 × g for 30 min at 4°C. The supernatant is collected into a chromatography column (Poly-Prep, Bio-Rad)

and it is incubated with 2 mL of His-select HC Nickel affinity gel (Sigma) previously treated as indicated by the supplier. The detergent-solubilised membranes are incubated with the resin overnight in a rocking well at 4°C. The next day, the material not-bound to the column is collected and the resin rinsed with 10 mL of washing buffer 1 (50 mM Tris-HCl, 150 mM NaCl, 5% glycerol, 0.1% DDM, 0.1% CHAPS, 0.02% CHS, 1 mM PMSF, 0.1 mM TCEP and 1 µL/mL of protease inhibitor cocktail and 10 mM imidazole), followed by 10 mL of washing buffer 2 (50 mM Tris-HCl, 150 mM NaCl, 5% glycerol, 0.1% DDM, 0.1% CHAPS, 0.02% CHS, 1 mM PMSF, 0.1 mM TCEP and 1 µL/mL of protease inhibitor cocktail and 20 mM imidazole). Such steps allow for non-specific bound protein to be eluted. To note that total detergent concentration is reduced by decreasing DDM from 1 to 0.1%. Detergent concentration decrease (with final concentration being still above the DDM CMC) facilitates the reconstitution process performed afterwards. To note also that ligand is now excluded from the buffer to avoid interference with the ligand binding assays performed afterwards. At this stage the one-pot purification and reconstitution protocol is applied. This consists in incubating the resin containing the detergent-solubilized CCR5 with 10 mL of SUVs at 1 mg/mL for 10 min. This process allows a first receptor incorporation. Following that the eluted solution is discarded and then the resin is incubated with 0.5 mL of 3 mg/mL SUVs in the presence of 200 mM imidazole for 40 min. SUV were prepared by tip sonication for 30 min after direct hydration of lipid films by buffer. At this stage the receptor is eluted from the resin in the liposome reconstituted form. To ascertain both lipid and protein presence in the sample pATR-FTIR experiments are conducted. The protein concentration in the sample is measured by BCA and protein purity and identity monitored by SDS gel electrophoresis and Western Blot analysis. To do so, samples were boiled 5 min in 1× loading buffer (0.06 M Tris-Cl pH 6.8, 2% SDS, 10% glycerol, 5% β-mercaptoethanol, 0.002% bromophenol blue), separated on a 12 % SDS-PAGE. Proteins were electrically transferred onto nitrocellulose membranes (Optitran BA-S83, Schleicher & Schuell) in the presence of transfer buffer (39 mM glycine, 48 mM Tris-base, 2% EtOH and 0.037% SDS) and were probed with monoclonal anti-His antibodies (Tebu). Peroxidase-conjugated anti-mouse antibodies (Sigma) were used as secondary antibodies. Binding was detected with the SuperSignal reagent (Pierce) and the Gnome Imaging system (Syngene).

pATR-FTIR measurements

ATR-FTIR spectra were recorded on a Nicolet 6700 FT-IR spectrometer (Nicolet Instrument, Madison,WI) equipped with a liquid nitrogen cooled mercury–cadmium–telluride detector (ThermoFisher Scientific, San Jose, CA, USA), with a spectral resolution of 4 cm^{-1} and a one-level zero filling. Proteolipid bilayers adsorbed on a germanium ATR crystal were obtained by spontaneous fusion of 20 µL of proteoliposomes (POPC/cholesterol 9/1 mol/mol) obtained after CCR5 reconstitution. Bilayer formation was monitored by following the intensity of the 2920 cm^{-1} band, that corresponds to the antisymmetric CH_2 fatty acid stretching bond. A value of about 1.5×10^{-3} is expected if a complete and single lipid bilayer is assembled. When this value was reached the sample was thoroughly washed with buffer (50 mM Tris-HCl, 150 mM NaCl) to remove excess of proteoliposomes and detergent traces. Since ATR spectroscopy is sensitive to the orientation of the lipid and peptide [62], spectra were recorded with a parallel (*p*) and perpendicular (*s*) polarization of the incident light. All the orientation information is then contained in the dichroic ratio $R_{ATR} = Ap/As$, where Ap and As represent the absorbance of the considered band for the p or s polarization of the incident light, respectively (for more details see [63]).

Cell-free expression of CCR5 and reconstitution on liposomes

Liposome preparation

Liposomes were prepared using a 10 mg/mL lipid mixture of 1,2-Dioleoyl-sn-glycero-3-phosphocholine (DOPC), 1,2-dioleoyl-sn-glycero-3-phosphoethanolamine (DOPE) and 1,2-dimyristoyl-sn-glycero-3-phosphatidic acid (DMPA) with or without cholesterol. Then, these lipids were purchased as the chloroform solution from Avanti Polar Lipids (Alabaster, AL, USA). Chloroform evaporated using a Uniequip vacuum centrifuge (Univapo 150H). The thin lipid film was rehydrated with 50 mM HEPES pH 7.5 to obtain 30 mg/mL lipid slurry. This solution was sonicated using a tip sonicator (Branson Digital Sonifier 250) at 20% for 30 s five times and filtered (0.22 µm polyethersulfone [PES] filter) to preform liposomes.

Cell-free expression and purification of CCR5 proteoliposomes

CCR5 cDNA sequence was sub-cloned into a specific plasmid, optimized by Synthelis SAS. The plasmid and the preformed liposomes solution were added to 1 mL of the batch reaction mixture. The energy regeneration system (NTPs, salts, amino acids, chaperones, cofactors, etc) was developed by Synthelis SAS. Different concentrations of magnesium (0–50 mM) and potassium (0–320 mM) were tested to optimize the protein expression. Cell-free reaction was carried out at 30°C for 16 h with gentle agitation at 400 rpm using an *Escherichia coli* S30 extract. To purify these proteoliposomes, cell-free reactions were loaded on top of a three-step discontinuous sucrose gradient (60%, 30% and 5%) prepared in 50 mM HEPES pH 7.5 buffer. After centrifugation at 280,000 x *g* for 1 h at 4°C, fractions were collected at each interface. Then they were analyzed by Western blotting using a poly histidine antibody conjugated with a horseradish peroxidase (Sigma-Aldrich) diluted at 1:10 000 in TBS-Tween buffer, 5% nonfat milk and by Coomassie blue. Proteoliposomes were stored at −80°C until use.

Ligand binding affinity measurements to CCR5 proteolipid model systems – fluorescence anisotropy

To investigate the activity of the CCR5 receptor following isolation, purification and reconstitution procedures and also to investigate the role of lipids in the receptor/ligand affinity, FA was applied. To do so, it is important that proteoliposomes are quite homogeneous, thus passing them though an extruder equipped with a 100 nm filter (Avanti Polar Lipids) can be advantageous. The ligand competition assays are performed in black flat bottom and non-binding 96-well plates (Greiner) by incubating a fixed concentration of proteoliposomes with a fixed concentration of DAPTA-FITC (10 nM), a potent CCR5 antagonist (Selleckchem) and a variable concentration of maraviroc, ranging from 10^{-4} to 10^{-13}M. The experiment is performed in an ice bath. Fluorescence anisotropy is measured in a 96 well plate reader equipped with polarizer (Clariostar, BMG Labtech) with an excitation wavelength at 470 nm and emission at 515 nm, and an excitation band of 5 nm. Data is analyzed and plotted using Graph Pad Prism. Data is fitted using a non-linear one-site competition that allows the IC_{50} (ligand concentration that displaces 50% of the fluorescently labelled ligand) to be determined. Each experiment was performed at least three times from different proteoliposome preparations.

Ligand binding affinity measurements to CCR5 proteolipid model systems – PWR

PWR experiments were performed on a homemade instrument that had a spectral angular resolution of ≥ 0.5 mdeg. Resonances can be obtained with light whose electric vector is either parallel (*s*-polarization) or perpendicular (*p*-polarization) to the plane of the resonator surface. The principles behind the technique and information obtained have been reported elsewhere (see *e.g.* [36, 64-66]). The sample to be analyzed (a proteolipid membrane containing the CCR5 receptor) was made by incubation of proteoliposomes with the sensor surface (a BK7 prism coated with silver and over coated with silica) leading to spontaneous burst of the liposomes to form a planar bilayer. Bilayer formation is followed by both the changes in magnitude of the spectral changes in both polarizations (informative about the mass gain that occurs upon the fusion process) and the anisotropy signal that is indicative of lipid orientation and membrane ordering. To note that prior to spectra are acquired for the buffer (50 mM Tris-HCl, 150 mM NaCl) alone (blank). The method used to prepare the lipid bilayer is based on the procedure by Mueller and Rudin [67] to make black lipid membranes across a small hole in a Teflon block, the method has been reported [64, 68]. After bilayer formation, maraviroc was incrementally added to the cell sample compartment and the spectral changes monitored with both polarizations. Affinities between the peptide and the lipids were obtained by plotting the PWR spectral changes that occur upon incremental additions of ligand to the cell. Data fitting (GraphPad Prism) through a hyperbolic saturation curve provides the apparent dissociation constants.

CGMDS

CCR5 structure used in this study was retrieved from Tan *et al*. article (PDB entry : 4MBS)[6]. Missing atoms were added with Discovery Studio3.1 (Dassault Systems, BIOVIA, San Diego: Dassault Systems, 2011) and the full protein was minimized.

This structure was converted in a CG model using the martinize protocol as described on Martini website (http: //www.cgmartini.nl) with the application of an elastic network. Molecular dynamics simulations (MDS) were performed with GROMACS version 5.1.4 package [69, 70], with standard settings associated with the MARTINI V2.2 coarse-grain force field [71-73]. Two systems were

studied where CCR5 is embedded at the center of a preformed membrane in a quadratic box composed of: *i)* POPC and *ii)* POPC with 10 % of cholesterol. Membranes were pre-assembled using the Insane Script [74]. Dynamics were done in aqueous medium standard CG water) with 0.15 M NaCl for ionic strength and two replicas of each system were simulated for 4 μs each. After energy minimization, the system was simulated with a time step of 20 fs in the isothermal-isobaric ensemble. The temperature was kept constant using V-rescale thermostat at 310 K with a coupling constant τp = 4.0 ps [75] and the pressure was semi-isotropically maintained constant at 1 bar using the Berendsen barostat [76] for equilibration step, then coupled to an external bath of P = 1 bar with a coupling constant of τp = 12 ps and compressability of $\chi = 3.0 \times 10^{-4}$ bar^{-1} using Parrinello-Rahman barostat [77]. Electrostatics interactions shifted to zero in the range of 0-1.1 nm and a dielectric constant of 15. Van der Waals interactions were ignored when exceeding the limit distance (cutoff = 1.1 nm).

The protein dynamics and flexibility were analyzed by calculating the root mean square deviation (RMSD) of CCR5 over time in each simulation and the preferentially helices contacted by cholesterol were determined by computing the radial distribution functions (RDF) of cholesterol molecules relative to each helix.

Author contributions

PC, CC, SC, MV, NC, RB and IDA performed the experiments. PC, CC, SC, MV, SL, BT and IDA analyzed the data. IDA wrote the manuscript with contributions from all the authors.

Acknowledgments

The authors acknowledge Renaud Wagner (U. of Strasbourg, France) for the *Pichia pastoris* vector pPIC9K used for the expression of CCR5 and Nuska Tschammer (U. of Erlangen, Germany) for the cDNA of CCR5.

La ligue contre le cancer is acknowledged by partially funding the project.

Disclosure of conflicts of interest

The authors declare no conflict of interest.

References

1. Alkhatib, G. (2009) The biology of CCR5 and CXCR4, *Curr Opin HIV AIDS.* **4**, 96-103.

2. Choi, W. T. & An, J. (2011) Biology and clinical relevance of chemokines and chemokine receptors CXCR4 and CCR5 in human diseases, *Exp Biol Med (Maywood).* **236**, 637-47.

3. Scholten, D. J., Wijtmans, M., van Senten, J. R., Custers, H., Stunnenberg, A., de Esch, I. J., Smit, M. J. & Leurs, R. (2015) Pharmacological characterization of [3H]VUF11211, a novel radiolabeled small-molecule inverse agonist for the chemokine receptor CXCR3, *Molecular pharmacology.* **87**, 639-48.

4. Wood, A. & Armour, D. (2005) The discovery of the CCR5 receptor antagonist, UK-427,857, a new agent for the treatment of HIV infection and AIDS, *Prog Med Chem.* **43**, 239-71.

5. Shaik, M. M., Peng, H., Lu, J., Rits-Volloch, S., Xu, C., Liao, M. & Chen, B. (2019) Structural basis of coreceptor recognition by HIV-1 envelope spike, *Nature.* **565**, 318-323.

6. Tan, Q., Zhu, Y., Li, J., Chen, Z., Han, G. W., Kufareva, I., Li, T., Ma, L., Fenalti, G., Zhang, W., Xie, X., Yang, H., Jiang, H., Cherezov, V., Liu, H., Stevens, R. C., Zhao, Q. & Wu, B. (2013) Structure of the CCR5 chemokine receptor-HIV entry inhibitor maraviroc complex, *Science.* **341**, 1387-90.

7. Oates, J. & Watts, A. (2011) Uncovering the intimate relationship between lipids, cholesterol and GPCR activation, *Curr Opin Struct Biol.* **21**, 802-7.

8. Bjork, K. & Svenningsson, P. (2011) Modulation of monoamine receptors by adaptor proteins and lipid rafts: role in some effects of centrally acting drugs and therapeutic agents, *Annual review of pharmacology and toxicology.* **51**, 211-42.

9. Ostrom, R. S. & Insel, P. A. (2004) The evolving role of lipid rafts and caveolae in G protein-coupled receptor signaling: implications for molecular pharmacology, *Br J Pharmacol.* **143**, 235-45.

10. Barnett-Norris, J., Lynch, D. & Reggio, P. H. (2005) Lipids, lipid rafts and caveolae: their importance for GPCR signaling and their centrality to the endocannabinoid system, *Life sciences.* **77**, 1625-39.

11. Nguyen, D. H., Giri, B., Collins, G. & Taub, D. D. (2005) Dynamic reorganization of chemokine receptors, cholesterol, lipid rafts, and adhesion molecules to sites of CD4 engagement, *Exp Cell Res.* **304**, 559-69.

12. Ablan, S., Rawat, S. S., Viard, M., Wang, J. M., Puri, A. & Blumenthal, R. (2006) The role of cholesterol and sphingolipids in chemokine receptor function and HIV-1 envelope glycoprotein-mediated fusion, *Virol J.* **3**, 104.

13. Rose, J. J., Foley, J. F., Yi, L., Herren, G. & Venkatesan, S. (2008) Cholesterol is obligatory for polarization and chemotaxis but not for endocytosis and associated signaling from chemoattractant receptors in human neutrophils, *J Biomed Sci.* **15**, 441-61.

14. Chinni, S. R., Yamamoto, H., Dong, Z., Sabbota, A., Bonfil, R. D. & Cher, M. L. (2008) CXCL12/CXCR4 transactivates HER2 in lipid rafts of prostate cancer cells and promotes growth of metastatic deposits in bone, *Mol Cancer Res.* **6**, 446-57.

15. Cardaba, C. M., Kerr, J. S. & Mueller, A. (2008) CCR5 internalisation and signalling have different dependence on membrane lipid raft integrity, *Cell Signal.* **20**, 1687-94.

16. Finnegan, C. M., Rawat, S. S., Puri, A., Wang, J. M., Ruscetti, F. W. & Blumenthal, R. (2004) Ceramide, a target for antiretroviral therapy, *Proceedings of the National Academy of Sciences of the United States of America.* **101**, 15452-7.

17. Zidovetzki, R. & Levitan, I. (2007) Use of cyclodextrins to manipulate plasma membrane cholesterol content: evidence, misconceptions and control strategies, *Biochimica et biophysica acta.* **1768**, 1311-24.

18. Maziere, C., Conte, M. A., Degonville, J., Ali, D. & Maziere, J. C. (1999) Cellular enrichment with polyunsaturated fatty acids induces an oxidative stress and activates the transcription factors AP1 and NFkappaB, *Biochemical and biophysical research communications.* **265**, 116-22.

19. Hirz, M., Richter, G., Leitner, E., Wriessnegger, T. & Pichler, H. (2013) A novel cholesterol-producing Pichia pastoris strain is an ideal host for functional expression of human Na,K-ATPase alpha3beta1 isoform, *Appl Microbiol Biotechnol.* **97**, 9465-78.

20. Tucker, J. & Grisshammer, R. (1996) Purification of a rat neurotensin receptor expressed in Escherichia coli, *The Biochemical journal.* **317 (Pt 3)**, 891-9.

21. Weiss, H. M. & Grisshammer, R. (2002) Purification and characterization of the human adenosine A(2a) receptor functionally expressed in Escherichia coli, *European journal of biochemistry / FEBS.* **269**, 82-92.

22. Jaakola, V. P., Griffith, M. T., Hanson, M. A., Cherezov, V., Chien, E. Y., Lane, J. R., Ijzerman, A. P. & Stevens, R. C. (2008) The 2.6 angstrom crystal structure of a human A2A adenosine receptor bound to an antagonist, *Science.* **322**, 1211-7.

23. Nasrallah, C., Rottier, K., Marcellin, R., Compan, V., Font, J., Llebaria, A., Pin, J. P., Baneres, J. L. & Lebon, G. (2018) Direct coupling of detergent purified human mGlu5 receptor to the heterotrimeric G proteins Gq and Gs, *Sci Rep.* **8**, 4407.

24. Mirzabekov, T., Bannert, N., Farzan, M., Hofmann, W., Kolchinsky, P., Wu, L., Wyatt, R. & Sodroski, J. (1999) Enhanced expression, native purification, and characterization of CCR5, a principal HIV-1 coreceptor, *The Journal of biological chemistry.* **274**, 28745-50.

25. Samson, M., Labbe, O., Mollereau, C., Vassart, G. & Parmentier, M. (1996) Molecular cloning and functional expression of a new human CC-chemokine receptor gene, *Biochemistry.* **35**, 3362-7.

26. Mirzabekov, T., Kontos, H., Farzan, M., Marasco, W. & Sodroski, J. (2000) Paramagnetic proteoliposomes containing a pure, native, and oriented seven-transmembrane segment protein, CCR5, *Nature biotechnology.* **18**, 649-54.

27. Devesa, F., Chams, V., Dinadayala, P., Stella, A., Ragas, A., Auboiroux, H., Stegmann, T. & Poquet, Y. (2002) Functional reconstitution of the HIV receptors CCR5 and CD4 in liposomes, *European journal of biochemistry / FEBS.* **269**, 5163-74.

28. Rigaud, J. L. & Levy, D. (2003) Reconstitution of membrane proteins into liposomes, *Methods Enzymol.* **372**, 65-86.

29. Klammt, C., Schwarz, D., Eifler, N., Engel, A., Piehler, J., Haase, W., Hahn, S., Dotsch, V. & Bernhard, F. (2007) Cell-free production of G protein-coupled receptors for functional and structural studies, *Journal of structural biology.* **158**, 482-93.

30. Yang, J. P., Cirico, T., Katzen, F., Peterson, T. C. & Kudlicki, W. (2011) Cell-free synthesis of a functional G protein-coupled receptor complexed with nanometer scale bilayer discs, *BMC Biotechnol.* **11**, 57.

31. Ishihara, G., Goto, M., Saeki, M., Ito, K., Hori, T., Kigawa, T., Shirouzu, M. & Yokoyama, S. (2005) Expression of G protein coupled receptors in a cell-free translational system using detergents and thioredoxin-fusion vectors, *Protein expression and purification.* **41**, 27-37.

32. Cortes, S., Barette, C., Beroud, R., De Waard, M. & Schaack, B. (2018) Functional characterization of cell-free expressed Kv1.3 channel using a voltage-sensitive fluorescent dye, *Protein expression and purification.* **145**, 94-99.

33. Calmet, P., De Maria, M., Harte, E., Lamb, D., Serrano-Vega, M., Jazayeri, A., Tschammer, N. & Alves, I. D. (2016) Real time monitoring of membrane GPCR reconstitution by plasmon waveguide resonance: on the role of lipids, *Sci Rep.* **6**, 36181.

34. Alves, I. D., Cowell, S. M., Salamon, Z., Devanathan, S., Tollin, G. & Hruby, V. J. (2004) Different structural states of the proteolipid membrane are produced by ligand binding to the human delta-opioid receptor as shown by plasmon-waveguide resonance spectroscopy, *Molecular pharmacology.* **65**, 1248-57.

35. Boye, K., Billottet, C., Pujol, N., Alves, I. D. & Bikfalvi, A. (2017) Ligand activation induces different conformational changes in CXCR3 receptor isoforms as evidenced by plasmon waveguide resonance (PWR), *Sci Rep.* **7**, 10703.

36. Alves, I. D. & Lecomte, S. (2019) Study of G-Protein Coupled Receptor Signaling in Membrane Environment by Plasmon Waveguide Resonance, *Acc Chem Res.* **52**, 1059-1067.

37. Dorr, P., Westby, M., Dobbs, S., Griffin, P., Irvine, B., Macartney, M., Mori, J., Rickett, G., Smith-Burchnell, C., Napier, C., Webster, R., Armour, D., Price, D., Stammen, B., Wood, A. & Perros, M. (2005) Maraviroc (UK-427,857), a potent, orally bioavailable, and selective small-molecule inhibitor of chemokine receptor CCR5 with broad-spectrum anti-human immunodeficiency virus type 1 activity, *Antimicrobial agents and chemotherapy.* **49**, 4721-32.

38. Rinken, A., Lavogina, D. & Kopanchuk, S. (2018) Assays with Detection of Fluorescence Anisotropy: Challenges and Possibilities for Characterizing Ligand Binding to GPCRs, *Trends in pharmacological sciences.* **39**, 187-199.

39. Castano, S. & Desbat, B. (2005) Structure and orientation study of fusion peptide FP23 of gp41 from HIV-1 alone or inserted into various lipid membrane models (mono-, bi- and multibi-layers) by FT-IR spectroscopies and Brewster angle microscopy, *Biochimica et biophysica acta.* **1715**, 81-95.

40. Mohole, M., Prasanna, X., Sengupta, D. & Chattopadhyay, A. (2018) Molecular Signatures of Cholesterol Interaction with Serotonin Receptors, *Adv Exp Med Biol.* **1112**, 151-160.

41. Sengupta, D. & Chattopadhyay, A. (2015) Molecular dynamics simulations of GPCR-cholesterol interaction: An emerging paradigm, *Biochimica et biophysica acta.* **1848**, 1775-82.

42. Manna, M., Niemela, M., Tynkkynen, J., Javanainen, M., Kulig, W., Muller, D. J., Rog, T. & Vattulainen, I. (2016) Mechanism of allosteric regulation of beta2-adrenergic receptor by cholesterol, *Elife.* **5** e18432.

43. Gimpl, G. (2016) Interaction of G protein coupled receptors and cholesterol, *Chemistry and physics of lipids.* **199**, 61-73.

44. Zhukovsky, M. A., Lee, P. H., Ott, A. & Helms, V. (2013) Putative cholesterol-binding sites in human immunodeficiency virus (HIV) coreceptors CXCR4 and CCR5, *Proteins.* **81**, 555-67.

45. Gahbauer, S., Pluhackova, K. & Bockmann, R. A. (2018) Closely related, yet unique: Distinct homo- and heterodimerization patterns of G protein coupled chemokine receptors and their fine-tuning by cholesterol, *PLoS Comput Biol.* **14**, e1006062.

46. Guixa-Gonzalez, R., Albasanz, J. L., Rodriguez-Espigares, I., Pastor, M., Sanz, F., Marti-Solano, M., Manna, M., Martinez-Seara, H., Hildebrand, P. W., Martin, M. & Selent, J. (2017) Membrane cholesterol access into a G-protein-coupled receptor, *Nat Commun.* **8**, 14505.

47. Lyman, E., Higgs, C., Kim, B., Lupyan, D., Shelley, J. C., Farid, R. & Voth, G. A. (2009) A role for a specific cholesterol interaction in stabilizing the Apo configuration of the human A(2A) adenosine receptor, *Structure.* **17**, 1660-1668.

48. Pluhackova, K., Gahbauer, S., Kranz, F., Wassenaar, T. A. & Bockmann, R. A. (2016) Dynamic Cholesterol-Conditioned Dimerization of the G Protein Coupled Chemokine Receptor Type 4, *PLoS Comput Biol.* **12**, e1005169.

49. Prasanna, X., Sengupta, D. & Chattopadhyay, A. (2016) Cholesterol-dependent Conformational Plasticity in GPCR Dimers, *Sci Rep.* **6**, 31858.

50. Song, W., Yen, H. Y., Robinson, C. V. & Sansom, M. S. P. (2019) State-dependent Lipid Interactions with the A2a Receptor Revealed by MD Simulations Using In Vivo-Mimetic Membranes, *Structure.* **27**, 392-403 e3.

51. Signoret, N., Hewlett, L., Wavre, S., Pelchen-Matthews, A., Oppermann, M. & Marsh, M. (2005) Agonist-induced endocytosis of CC chemokine receptor 5 is clathrin dependent, *Mol Biol Cell.* **16**, 902-17.

52. Nguyen, D. H. & Taub, D. (2002) Cholesterol is essential for macrophage inflammatory protein 1 beta binding and conformational integrity of CC chemokine receptor 5, *Blood.* **99**, 4298-306.

53. Muth, S., Fries, A. & Gimpl, G. (2011) Cholesterol-induced conformational changes in the oxytocin receptor, *The Biochemical journal.* **437**, 541-53.

54. Nguyen, D. H. & Taub, D. D. (2003) Inhibition of chemokine receptor function by membrane cholesterol oxidation, *Exp Cell Res.* **291**, 36-45.

55. Berro, R., Klasse, P. J., Lascano, D., Flegler, A., Nagashima, K. A., Sanders, R. W., Sakmar, T. P., Hope, T. J. & Moore, J. P. (2011) Multiple CCR5 conformations on the cell surface are used differentially by human immunodeficiency viruses resistant or sensitive to CCR5 inhibitors, *Journal of virology.* **85**, 8227-40.

56. Garcia-Perez, J., Rueda, P., Alcami, J., Rognan, D., Arenzana-Seisdedos, F., Lagane, B. & Kellenberger, E. (2011) Allosteric model of maraviroc binding to CC chemokine receptor 5 (CCR5), *The Journal of biological chemistry.* **286**, 33409-21.

57. Bertheleme, N., Singh, S., Dowell, S. & Byrne, B. (2015) Heterologous expression of G-protein-coupled receptors in yeast, *Methods Enzymol.* **556**, 141-64.

58. Logez, C., Alkhalfioui, F., Byrne, B. & Wagner, R. (2012) Preparation of Pichia pastoris expression plasmids, *Methods Mol Biol.* **866**, 25-40.
59. Andre, N., Cherouati, N., Prual, C., Steffan, T., Zeder-Lutz, G., Magnin, T., Pattus, F., Michel, H., Wagner, R. & Reinhart, C. (2006) Enhancing functional production of G protein-coupled receptors in Pichia pastoris to levels required for structural studies via a single expression screen, *Protein science : a publication of the Protein Society.* **15**, 1115-26.
60. McGraw, C., Yang, L., Levental, I., Lyman, E. & Robinson, A. S. (2019) Membrane cholesterol depletion reduces downstream signaling activity of the adenosine A2A receptor, *Biochim Biophys Acta Biomembr.* **1861**, 760-767.
61. Wu, S. & Letchworth, G. J. (2004) High efficiency transformation by electroporation of Pichia pastoris pretreated with lithium acetate and dithiothreitol, *Biotechniques.* **36**, 152-4.
62. Goormaghtigh, E., Raussens, V. & Ruysschaert, J. M. (1999) Attenuated total reflection infrared spectroscopy of proteins and lipids in biological membranes, *Biochim Biophys Acta.* **1422**, 105-85.
63. Castano, S. & Desbat, B. (2005) Structure and orientation study of fusion peptide FP23 of gp41 from HIV-1 alone or inserted into various lipid membrane models (mono-, bi- and multibi-layers) by FT-IR spectroscopies and Brewster angle microscopy, *Biochim Biophys Acta.* **1715**, 81-95.
64. Salamon, Z., Macleod, H. A. & Tollin, G. (1997) Coupled plasmon-waveguide resonators: a new spectroscopic tool for probing proteolipid film structure and properties, *Biophys J.* **73**, 2791-7.
65. Alves, I. D., Park, C. K. & Hruby, V. J. (2005) Plasmon resonance methods in GPCR signaling and other membrane events, *Current protein & peptide science.* **6**, 293-312.
66. Harte, E., Maalouli, N., Shalabney, A., Texier, E., Berthelot, K., Lecomte, S. & Alves, I. D. (2014) Probing the kinetics of lipid membrane formation and the interaction of a nontoxic and a toxic amyloid with plasmon waveguide resonance, *Chem Commun.* **50**, 4168-71.
67. Mueller, P. & Rudin, D. O. (1968) Resting and action potentials in experimental bimolecular lipid membranes, *J Theor Biol.* **18**, 222-58.
68. Alves, I. D., Salamon, Z., Varga, E., Yamamura, H. I., Tollin, G. & Hruby, V. J. (2003) Direct observation of G-protein binding to the human delta-opioid receptor using plasmon-waveguide resonance spectroscopy, *J Biol Chem.* **278**, 48890-7.
69. Van Der Spoel, D., Lindahl, E., Hess, B., Groenhof, G., Mark, A. E. & Berendsen, H. J. (2005) GROMACS: fast, flexible, and free, *J Comput Chem.* **26**, 1701-18.

70. Pronk, S., Pall, S., Schulz, R., Larsson, P., Bjelkmar, P., Apostolov, R., Shirts, M. R., Smith, J. C., Kasson, P. M., van der Spoel, D., Hess, B. & Lindahl, E. (2013) GROMACS 4.5: a high-throughput and highly parallel open source molecular simulation toolkit, *Bioinformatics.* **29**, 845-54.
71. Monticelli, L., Kandasamy, S. K., Periole, X., Larson, R. G., Tieleman, D. P. & Marrink, S. J. (2008) The MARTINI Coarse-Grained Force Field: Extension to Proteins, *J Chem Theory Comput.* **4**, 819-34.
72. Marrink, S. J., Risselada, H. J., Yefimov, S., Tieleman, D. P. & de Vries, A. H. (2007) The MARTINI force field: coarse grained model for biomolecular simulations, *The journal of physical chemistry B.* **111**, 7812-24.
73. de Jong, D. H., Singh, G., Bennett, W. F., Arnarez, C., Wassenaar, T. A., Schafer, L. V., Periole, X., Tieleman, D. P. & Marrink, S. J. (2013) Improved Parameters for the Martini Coarse-Grained Protein Force Field, *J Chem Theory Comput.* **9**, 687-97.
74. Wassenaar, T. A., Ingolfsson, H. I., Bockmann, R. A., Tieleman, D. P. & Marrink, S. J. (2015) Computational Lipidomics with insane: A Versatile Tool for Generating Custom Membranes for Molecular Simulations, *J Chem Theory Comput.* **11**, 2144-55.
75. Bussi, G., Donadio, D. & Parrinello, M. (2007) Canonical sampling through velocity rescaling, *The Journal of chemical physics.* **126**, 014101.
76. Mavri, J. & Berendsen, H. J. (1994) Dynamical simulation of a quantum harmonic oscillator in a noble-gas bath by density-matrix evolution, *Phys Rev E Stat Phys Plasmas Fluids Relat Interdiscip Topics.* **50**, 198-204.
77. Piaggi, P. M. & Parrinello, M. (2018) Predicting polymorphism in molecular crystals using orientational entropy, *Proceedings of the National Academy of Sciences of the United States of America.* **115**, 10251-10256.

Figures legends

Figure 1. Characterization of CCR5 containing samples upon detergent-solubilisation and purification by Dot Blot (A) Western Blot (B) and SDS-electrophoresis (C). A) Crude extracts of 1) membrane fraction and 2) solubilized material; Fractions from IMAC column: 3) Flow through and 4) imidazole eluted fraction. B) 1) Crude membrane fraction; 2) Detergent solubilized membrane; 3) Imidazole eluted protein; 4) MW marker; C) 1) Imidazole eluted protein after IMAC; 2) MW marker.

Anti-His antibody was used for CCR5 detection in Dot Blot and Western Blot assays and silver staining was used for protein detection in SDS-electrophoresis. The experiment was repeated 2 times.

Figure 2. Determination of R_{sat} and R_{sol} for POPC and a mixture of detergent composed of DDM/CHAPS/CHS (0.1%/0.1%/0.02%). R_{sat} and R_{sol} were determined by measuring sample turbidity (Absorbance at 436 nm) at different lipid/detergent ratios. They correspond to the slope of the lines and were determined to be 0.97 ± 0.03 and 1.7 ± 0.08, respectively. The experiment was repeated two times.

Figure 3. Optimized production of CCR5 proteoliposomes using cell-free expression system. (A) Diagram of the production of CCR5 proteoliposomes by cell-free expression system. (B) Coomassie blue staining of CCR5 after purification of sucrose gradient. Lane 1, expression in the presence of liposomes with cholesterol; Lane 2, expression in the presence of liposomes without cholesterol; Lane 3, molecular weight markers; Lanes 4-7: BSA (C) Western-blot analysis of CCR5 proteoliposomes, using monoclonal anti-histidine antibodies. Lane 1, expression in the presence of liposomes with cholesterol; Lane 2, expression in the presence of liposomes without cholesterol. The experiment was repeated two times.

Figure 4. Response of CCR5 obtained from *P. pastoris* and reconstituted in a POPC lipid model system to maraviroc, followed by PWR (A, B, C) and Fluorescence Anisotropy (D). (A and B) PWR spectra of the buffer (black), after formation of a proteolipid membrane (blue) and following addition of saturating concentration of ligand maraviroc (red) obtained for *p*- and *s*-pol, respectively. (C) Binding curve obtained from the resonance shifts in PWR upon increasing ligand concentration of maraviroc to the proteolipid membrane deposited in the PWR sensor. K_D value was obtained from data fit to a classical one site hyperbolic binding curve. Average K_D values from three independent experiments are presented in Fig 7B. (D) Binding competition between a fluorescent CCR5 agonist (DAPTA-FITC, fixed concentration of 10 nM) and maraviroc (concentration ranging from 1×10^{-13} to 1×10^{-4} M) to CCR5-containing proteoliposomes followed by Fluorescence Anisotropy. The IC_{50}

value was determined using a classical one site binding inhibition curve. Average IC_{50} values from three independent experiments are provided in Fig. 7A.

Figure 5. Response of CCR5 obtained from *P. pastoris* expression and reconstituted in a POPC/chol (9/1 mol/mol) lipid model system to maraviroc, followed by PWR (A, B) and Fluorescence Anisotropy (C). (A, B) PWR spectra of buffer (black), a POPC/chol proteolipid membrane containing CCR5 (blue) and upon addition of saturating concentrations of maraviroc (red dotted line). (C) Binding competition between a fluorescent CCR5 agonist (DAPTA-FITC, fixed concentration of 10 nM) and maraviroc (concentration ranging from 1×10^{-12} to 1×10^{-4} M) followed by Fluorescence Anisotropy. Average IC_{50} values from three independent experiments are provided in Fig. 7A.

Figure 6. pATR-FTIR spectra of a proteolipid membrane (POPC/chol 9/1 mol/mol) containing CCR5 showing both lipid and protein expected contributions. The high wavenumber region (Panel A) is known to be the adsorption band of the CH_2 vibration modes characteristic of the lipid bilayer acyl chain. The range 1700-1500 cm^{-1} is the signature of the amide groups from the protein. The ratio of the *p*-polarized light spectrum (red) and *s*-polarized light spectrum (blue) allows to determine the orientation of the α-helices of the protein present in the bilayer. The experiment was repeated two times.

Figure 7. Impact of cholesterol (10% of the total lipids) in the binding affinity of maraviroc to the CCR5 obtained from *P. pastoris* expression and reconstituted in proteoliposomes (A) or a planar lipid bilayer (B). Data represent the results of three independent experiments. The mean IC_{50} values and respective standard deviation (SD) are 23 ± 8 nM and 0.69 ± 0.12 nM, for the experiment in the presence and in the absence of cholesterol. The average K_D value and respective standard deviation in the absence of cholesterol is 0.65 ± 0.23 nM. To note that as there are no PWR spectral changes upon maraviroc addition to the CCR5 in a membrane in the presence of cholesterol, no affinity was possible to be determined in this case.

Figure 8. Response of CCR5 obtained from cell-free expression and reconstituted in a lipid model system without (DOPC/DOPE/DMPA) or with cholesterol (DOPC/DOPE/DMPA/chol) to maraviroc, followed by PWR (A, B, C) and Fluorescence Anisotropy (D, E). (A, B) PWR spectra of buffer (black), a non-cholesterol proteolipid membrane containing CCR5 (blue) and upon addition of saturating concentrations of maraviroc (red).

(C) Binding curve obtained from the resonance shifts in PWR upon increasing ligand concentration of maraviroc to the proteolipid membrane deposited in the PWR sensor. K_D value was obtained from data fit to a classical one site hyperbolic binding curve. Average K_D values from three independent experiments are presented in Fig 9B. (D and E) Binding competition between a fluorescent CCR5 agonist (DAPTA-FITC, fixed concentration of 10 nM) and maraviroc (concentration ranging from 1×10^{-13} to 1×10^{-5} or 1×10^{-4} M) to the CCR5 reconstituted in the absence and in the presence of cholesterol, respectively and followed by Fluorescence Anisotropy. The IC_{50} value was determined using a classical one site binding inhibition curve. Average IC_{50} values from three independent experiments are provided in Fig. 9A.

Figure 9. Impact of cholesterol (30% of total lipids) in the binding affinity of maraviroc to the CCR5 obtained from cell-free expression and reconstituted in proteoliposomes (A) or a planar lipid bilayer (B). Data represent the results of three independent experiments. The mean IC_{50} values and respective standard deviation are $2.1 \times 10^{-7} \pm 2.8 \times 10^{-8}$ M and $6.7 \times 10^{-9} \pm 1.3 \times 10^{-9}$ M, for the experiment in the presence and in the absence of cholesterol. The average K_D value and respective standard deviations in the absence of cholesterol is 8.8 ± 1.5 nM. To note that as there are no PWR spectral changes upon maraviroc addition to the CCR5 in a membrane in the presence of cholesterol, no affinity was possible to be determined in this case.

Figure 10. Coarse grained initial system for MDS (*view from the extracellular side*). CCR5 is represented in pink cartoon for more clarity and helices are numbered in yellow. POPC lipids are in transparent dark blue and cholesterol appears in green (POPC:CHOL, 9:1). Water and ions beads were removed for more visibility. Molecular dynamics simulations (MDS) were performed with

GROMACS version 5.1.4 package, with standard settings associated with the MARTINI V2.2 coarse-grain force field (further details can be found in Materials and Methods).

Figure 11. Dynamics of CCR5 overtime in the absence and in the presence of cholesterol probed by CGMDS. (A) RMSD of the whole protein and (B) RMSD of the most dynamic helices (dark colors correspond to the results from CGMDS without cholesterol and light colors to the ones from CGMDS with 10 % cholesterol). Although there are no big changes in RMSD value for some helices, we can observe that the RMSD of helices in a cholesterol enriched membrane are still lower than the RMSD in a POPC membrane. Moreover, the light RMSD present less significant fluctuations attesting an increase of CCR5 rigidity. 3 different replicas were run. Molecular dynamics simulations (MDS) were performed with GROMACS version 5.1.4 package, with standard settings associated with the MARTINI V2.2 coarse-grain force field (further details can be found in Materials and Methods).

Figure 12. Radial distribution of cholesterol molecules relative to the different TM helices represented by different colors. A) All helices are represented. Helices VII, V, VI, IV and I displayed the greater interactions at closer range with cholesterol all along the simulation time. B) Specific TM segments are represented in different colors. To note that the pattern is slightly different than what was observed for the whole helices. Segments from helices I, IV, V, VI were found in proximity of cholesterol units, while TM VII segment was less concerned. The two panels depict the probability of presence of a cholesterol molecule at a definite distance from the helix center of mass. Molecular dynamics simulations (MDS) were performed with GROMACS version 5.1.4 package, with standard settings associated with the MARTINI V2.2 coarse-grain force field (further details can be found in Materials and Methods).

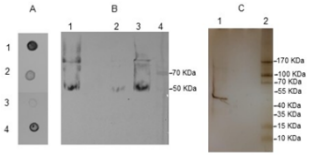

febs_15145_f1.tif

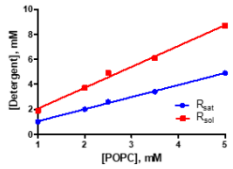

febs_15145_f2.tif

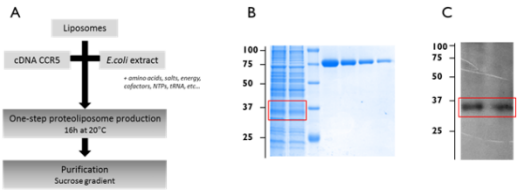

febs_15145_f3.tif

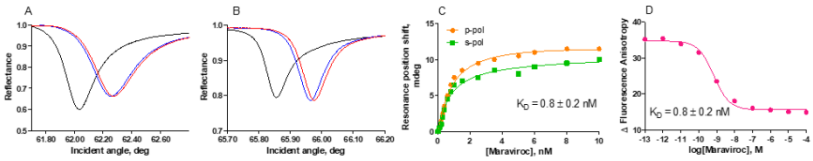

febs_15145_f4.tif

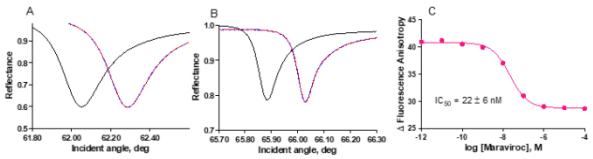

febs_15145_f5.tif

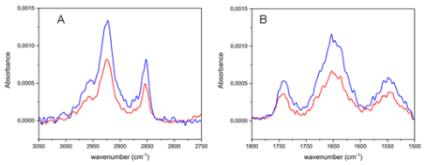

febs_15145_f6.tif

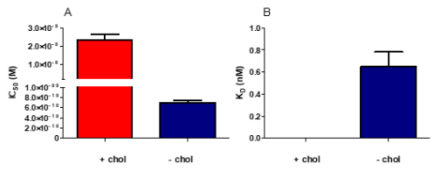

febs_15145_f7.tif

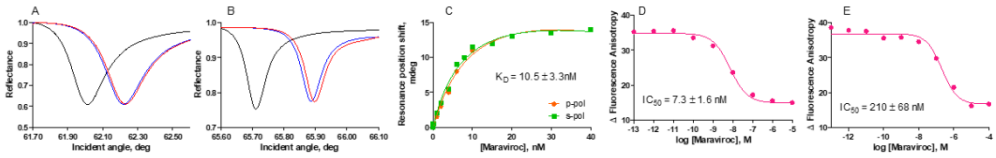

febs_15145_f8.tif

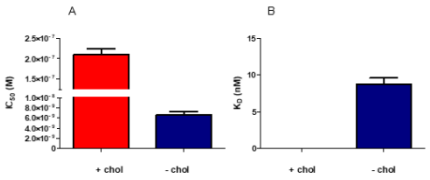

febs_15145_f9.tif

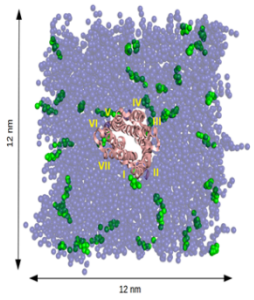

febs_15145_f10.tif

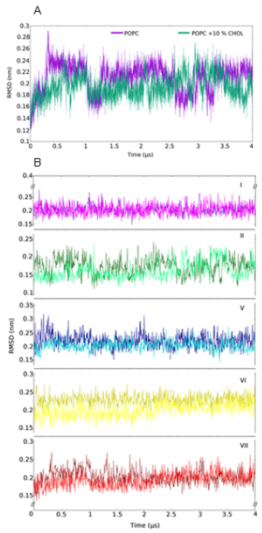

febs_15145_f11.tif

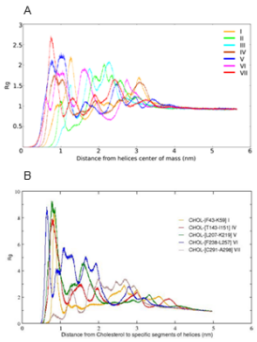

febs_15145_f12.tif